This is an open access article published under an ACS AuthorChoice License, which permits copying and redistribution of the article or any adaptations for non-commercial purposes.

ACS Macro Letters

Letter

pubs.acs.org/macroletters

Unlocking Chain Exchange in Highly Amphiphilic Block Polymer Micellar Systems: Influence of Agitation

Ryan P. Murphy,† Elizabeth G. Kelley,† Simon A. Rogers, Millicent O. Sullivan,* and Thomas H. Epps, III*

Department of Chemical and Biomolecular Engineering, University of Delaware, 150 Academy Street, Newark, Delaware 19716, United States

Supporting Information

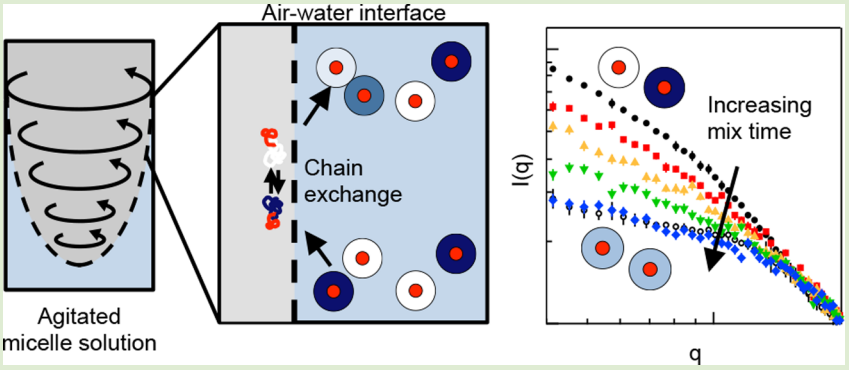

ABSTRACT: Chain exchange between block polymer micelles in highly selective solvents, such as water, is well-known to be arrested under quiescent conditions, yet this work demonstrates that simple agitation methods can induce rapid chain exchange in these solvents. Aqueous solutions containing either pure poly(butadiene-*b*-ethylene oxide) or pure poly(butadiene-*b*-ethylene oxide-d_4) micelles were combined and then subjected to agitation by vortex mixing, concentric cylinder Couette flow, or nitrogen gas sparging. Subsequently, the extent of chain exchange between micelles was quantified using small angle neutron scattering. Rapid vortex mixing induced chain exchange within minutes, as evidenced by a monotonic decrease in scattered intensity, whereas Couette flow and sparging did not lead to measurable chain exchange over the examined time scale of hours. The linear kinetics with respect to agitation time suggested a surface-limited exchange process at the air−water interface. These findings demonstrate the strong influence of processing conditions on block polymer solution assemblies.

The tunable self-assembly of amphiphilic block polymers has enabled bottom-up strategies for the design and fabrication of nanoscale particles in solution with distinct nanostructures and properties. Due to the versatility in polymer architectures and chemical functionalities, amphiphilic block polymers have been employed in various well-established applications including dispersants, cosmetics, and emulsifiers,[1,2] as well as in emerging areas such as nanoreactors,[3−5] diagnostic particles, and drug delivery vehicles.[5,6] A key challenge is that many developing technologies aim to encapsulate various cargoes such as catalysts, dyes, or drugs within the assembly, and encapsulation requires a fundamental understanding of molecular chain exchange dynamics to improve the performance, stability, and lifetime of the nanocarrier. Hindered chain exchange dynamics in selective solvents are known to produce kinetically trapped structures in which the size, morphology, and other functional properties of block polymer assemblies critically depend on sample preparation and processing conditions.[7−9] Fundamental investigations into chain exchange dynamics[10−16] and the influence of processing effects[17−25] (e.g., cosolvent addition and removal, mixing method, agitation rate) establish routes to create micelles with improved stability and provide insight into more complex, hierarchical assembly pathways.

Theoretical and experimental investigations of chain exchange in block polymer micelles show close agreement under quiescent conditions.[10−15] By employing time-resolved small angle neutron scattering (TR-SANS) and contrast-matching techniques to study block polymer structure and dynamics under equilibrium conditions, significant insight has been gained into the effects of core block molecular weight, molecular weight distribution, temperature, solvent selectivity, and solution-assembled morphology on chain exchange.[16] Despite the prevalence of agitation methods in block polymer assembly preparation, previous work has focused on equilibrium kinetics, and the influence of solution agitation on chain exchange has not been explored comprehensively.[26,27]

Received: July 18, 2014
Accepted: October 7, 2014
Published: October 14, 2014

 © 2014 American Chemical Society

The significant influence of shear and interfacial effects on nanoscale assemblies is evidenced by the considerable efforts to understand these phenomena in emulsions commonly found in pharmaceutical and personal care products[28,29] and in protein solutions used in the biopharmaceutical industry.[30−34] Micelle formulations developed for applications such as drug delivery or catalysis also are routinely subjected to agitation during processing, shipping, and usage, which could induce aggregation or undesirable changes in nanocarrier structure. For block polymer micelles, in particular, many investigations report the use of agitation during micelle preparation, yet only a few studies have systematically explored the effects of that agitation on the structure in the resulting assemblies.[17−23] One example for poly(styrene-*b*-2-vinylpyridine-*b*-ethylene oxide) triblock terpolymer micelles in water showed that discrete spherical micelles were formed at slower stir speeds, while cylindrical micelles and large aggregates were formed at faster stir speeds.[17] Similarly, Wang et al. demonstrated sphere-to-cylinder, sphere-to-vesicle, and cylinder-to-sphere transitions for poly(styrene-*b*-acrylic acid) diblock copolymer micelles in aqueous solution under high shear conditions imposed by a specially designed microfluidic mixing device.[21,22] Recently, the stirring of dilute aqueous solutions of poly(1,2-butadiene-*b*-ethylene oxide) (PB-PEO) diblock copolymer micelles was shown to induce micelle growth through a bimodal pathway following organic cosolvent removal.[24] Reports such as these demonstrate that nanocarrier stability can be influenced by solution agitation and underscore the need for quantitative investigations into the effects of mixing on chain exchange in block polymer solution assemblies.

Herein, contrast-matching SANS methods (Figure 1) that have been demonstrated in several other works[10−12,16,27,35−38] were used to quantify the fraction of chains exchanged between block polymer micelles as a result of mechanical mixing or solution agitation. PB-PEO has a very low critical micelle concentration (CMC) in water, on the order of 10^{-7} mol L^{-1},[39] and the resulting assemblies are reported to be kinetically trapped under quiescent conditions with no chain exchange occurring after several days due to highly unfavorable PB−water interactions ($\chi_{PB\text{-}water} \approx 3.5$).[26]

To examine the effects of solution agitation on chain exchange, aqueous solutions containing poly(1,2-butadiene-*b*-ethylene oxide) [PB-*h*PEO, M_n = 11.1 kg mol^{-1}, w_{hPEO} = 0.71, $Đ$ = 1.08] and poly(1,2-butadiene-*b*-ethylene oxide-d_4) [PB-*d*PEO, M_n = 11.0 kg mol^{-1}, w_{dPEO} = 0.71, $Đ$ = 1.09] micelles were prepared by dissolving the dry polymer powders in H_2O/D_2O mixtures. "Pre-mixed" micelle solutions containing micelles with randomly mixed *h*PEO/*d*PEO coronas were made to measure the scattering that would occur under conditions of complete chain exchange. These premixed solutions were prepared by blending 50 wt % PB-*h*PEO and 50 wt % PB-*d*PEO in benzene, freeze-drying, and dissolving the blended polymers in a 64 vol % D_2O/36 vol % H_2O mixture. The isotopic composition of the solvent was chosen to contrast-match the coronas of the premixed micelles. Meanwhile, for chain exchange measurements, separate solutions containing either pure PB-*h*PEO or pure PB-*d*PEO micelles in 64 vol % D_2O were combined at t_{mix} = 0 min. Subsequently, the solutions were agitated via rapid vortex mixing, concentric cylinder Couette flow, or nitrogen gas sparging (see Supporting Information for additional details) and then analyzed by SANS after a defined mix time (t_{mix}). Chain exchange between PB-*h*PEO and PB-*d*PEO micelles would decrease the scattering contrast and therefore the scattered intensity. Moreover, a decrease in the scattered intensity compared to that of the premixed micelle solution would be evidence of complete chain exchange.

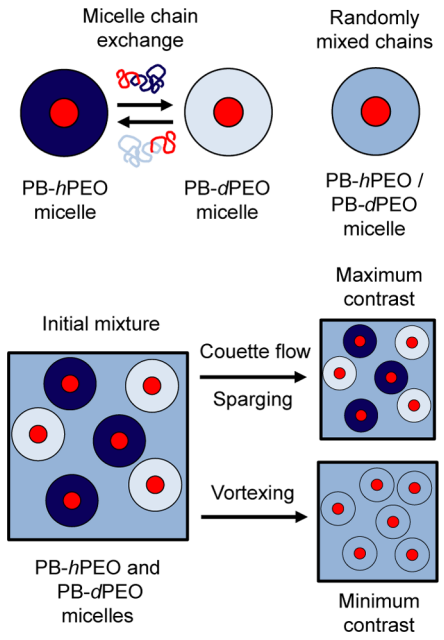

Figure 1. Schematic representation of contrast conditions used to study chain exchange as a result of solution agitation. Micelles containing nondeuterated PB chains in the core and either nondeuterated or deuterated PEO chains in the corona (lower left panel) were agitated using rapid vortex mixing, Couette flow, or nitrogen gas sparging. Subsequently, SANS was used to measure the scattering intensity as a function of mix time and, hence, to quantify the extent of chain exchange (lower right panels). Chain exchange between micelles decreases the solvent-corona contrast and the scattered intensity, and under certain agitation conditions, the scattered intensity gradually approaches that of micelles with randomly mixed *h*PEO/*d*PEO corona chains (minimum scattering contrast).

The extent of chain exchange can be related directly to the scattered intensity and can be defined by the relaxation function $R(t_{mix})$ given in eq 1.[10]

$$R(t_{mix}) = \left(\frac{I(t_{mix}) - I(\infty)}{I(0) - (\infty)}\right)^{1/2} \quad (1)$$

$I(\infty)$ and $I(0)$ are the integrated intensities for the premixed solution and the postmixed solution at t_{mix} = 0, respectively. $I(t_{mix})$ is the integrated intensity at a given mix time. An $R(t_{mix})$ value of 1 corresponds to no chain exchange, while a value of 0 corresponds to complete chain exchange or randomly mixed chains within micelles. Although the randomly mixed chains do not result in the full zero-average contrast condition (i.e., residual scattering exists from core−solvent and core−corona contrast), it was shown previously that residual scattering due to core contrast remained negligible at lower q-values.[11] Here, the scattered intensities were numerically integrated from 0.004 $Å^{-1} < q < 0.015$ $Å^{-1}$, over which the residual scattering due to the core contrast remained negligible.

SANS experiments were performed on the NG-7 30 m SANS Instrument at the National Institute of Standards and Technology (NIST) Center for Neutron Research (NCNR). After mixing the discrete samples, scattering data were acquired for 5 min and reduced using the standard procedures provided

dx.doi.org/10.1021/mz500435d | *ACS Macro Lett.* 2014, 3, 1106−1111

by NIST.[40] Time-resolved SANS techniques were not necessary for these mixing experiments as chain exchange between micelles did not occur during the quiescent acquisition conditions. Figure 2 presents the SANS data for micelle

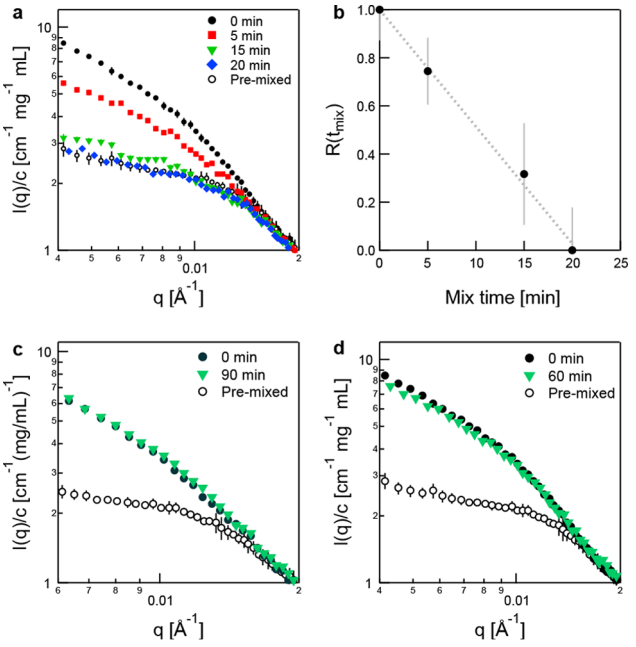

Figure 2. Chain exchange induced by solution agitation. (a) Rapid vortex mixing led to a decrease in scattered intensity. (b) The relaxation function $R(t_{mix})$ varied linearly as a function of mixing time. Negligible chain exchange was found after (c) 90 min Couette flow at 5000 s^{-1} and (d) 60 min of nitrogen gas sparging at 10 mL min^{-1}. The scattered intensities from SANS were normalized by polymer concentration. All agitated micelle solutions were prepared at 5.0 mg mL^{-1}. The maximum (0 min) and minimum (premixed) scattering curves are an average from three different concentrations. Error bars in (a), (c), and (d) represent the standard deviation in the measured scattered intensity. Error bars in (b) represent the propagated uncertainty in the normalized scattered intensity based on the uncertainty in polymer concentration.

solutions before and after various agitation methods. Note that each SANS curve represents an individual micelle solution mixed from t_{mix} = 0 min to the desired mix time. As shown in Figure 2a, the scattered intensity decreased as a result of rapid vortex mixing (analog setting 10, ~3200 rpm), showing that chain exchange could occur in as little as 5 min at the given agitation rate. Longer mixing durations further reduced the scattered intensity such that chain randomization within micelles was achieved after 20 min of mixing. Note that SANS and DLS experiments indicated that the vortex mixing did not lead to changes in the spherical core−shell micelle structure (see Supporting Information, Figures S1 and S2 and Tables S1 and S2), supporting the conclusion that the decrease in scattered intensity was due to chain exchange between micelles. Figure 2b shows that the fraction of chains exchanged varied linearly with mix time, which is highly suggestive of a surface-limited exchange rate. Other agitation methods including Couette flow at a high shear rate of 5000 s^{-1} for 90 min (Figure 2c) and nitrogen gas sparging at a flow rate of 10 mL min^{-1} for 60 min (Figure 2d) did not induce significant chain exchange over the examined mixing duration.

Comparing the results from the different agitation methods suggested that the vortex-induced chain exchange was facilitated by the rapid compression/expansion of the air−water interface. The lack of chain exchange during high shear conditions in the Couette cell implied that the exchange process was not exclusively a shear-induced effect, as Couette flow was estimated to have a similar volume average shear rate to vortex mixing but significantly different air−water interfacial contact.[31] In other words, shear forces (of the range applied herein) and imparted particle collisions alone were not sufficient to surmount the relatively large energetic barriers necessary for chain exchange between PB-PEO micelles in water.[26]

The interfacial argument is reasonable given the propensity for amphiphilic molecules to adsorb at interfaces. However, nitrogen gas sparging did not induce significant chain exchange after 60 min, even though full exchange was obtained after 20 min of vortex mixing. These two different outcomes likely were due to significant differences in air−water surface regeneration rates and volume average shear rates, both of which were estimated to be greater by a factor of ~10^2 for vortex mixing relative to sparging.[31] Recent studies on the same polymer system also showed that solution agitation via magnetic stirring did not lead to measurable chain exchange after 10 days.[24] Again, the surface regeneration rates were approximately 2 orders of magnitude greater during vortex mixing compared to magnetic stirring, emphasizing the importance of the air−water interface turnover. To further support the importance of the air−water contact, the air−solution volume ratio was reduced during vortex mixing (i.e., 4 mL of solution vs 1 mL of solution were loaded within equal-volume sealed vials), which resulted in considerably less chain exchange (see Supporting Information, Figure S3).

There are several reports illustrating the strong affinity of amphiphilic block polymers for the air−water interface.[41−43] In one example, Isa and co-workers studied the adsorption energies of PEO-based surfactants and showed that a PEO-containing block polymer adsorbed strongly to the air−water interface such that desorption was not detected under the experimental conditions.[43] These results suggest that block polymer amphiphiles only desorb from the interface at high surface pressures, such as the pressures created by shrinking and collapsing the interface. Given the importance of air−water contact for agitation-induced chain exchange and the expected high energy barrier to chain or micelle desorption, the results presented herein indicate that the interface must deform and be regenerated for chain exchange to occur. According to this hypothesis, the chain exchange would be limited by the available free air−water interface, which is consistent with the linear chain exchange rate.

SANS experiments were conducted at various polymer concentrations to examine the reproducibility of the linear chain exchange rate and to gain additional insight into the underlying exchange mechanisms. Figure 3 shows similar decreases in scattered intensity for micelle solutions exposed to rapid vortex mixing at polymer concentrations ranging from 2 to 15 mg mL^{-1}. Higher polymer concentrations required longer mix times to achieve micelles with randomly mixed chains. For example, randomly mixed micelles were obtained at t_{mix} ~ 10 min for the 2.4 mg mL^{-1} sample (Figure 3a), whereas the same degree of mixing took t_{mix} ~ 60 min for the 10.0 mg mL^{-1} sample (Figure 3c). The corresponding $R(t_{mix})$ for the different polymer concentrations decreased linearly with mix

dx.doi.org/10.1021/mz500435d | ACS Macro Lett. 2014, 3, 1106−1111

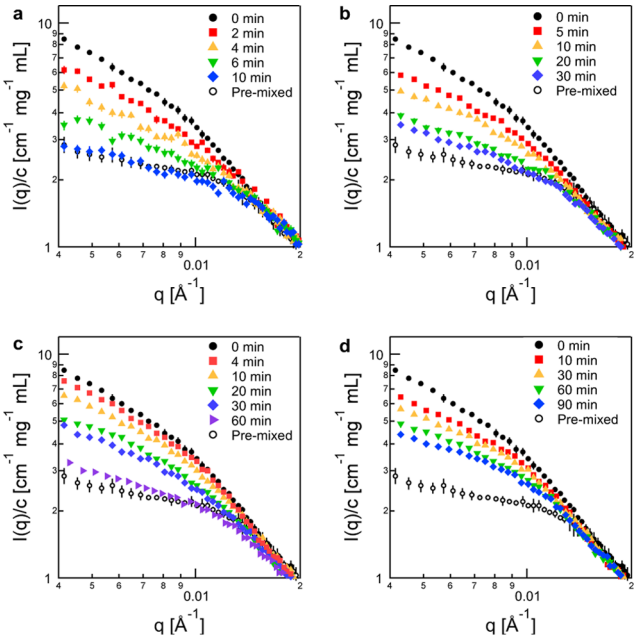

Figure 3. Concentration series for chain exchange induced by rapid vortex mixing. Scattered intensities from SANS were normalized by polymer concentration for (a) 2.4, (b) 7.5, (c) 10.0, and (d) 15.0 mg mL^{-1} micelle solutions at each given mix time (0 min up to 90 min). The 5.0 mg mL^{-1} data are presented in Figure 2. The normalized maximum (0 min) and minimum (premixed) scattering curves shown in (a–d) are the average curves obtained from samples at three different concentrations. Error bars represent the standard deviation in measured scattered intensity.

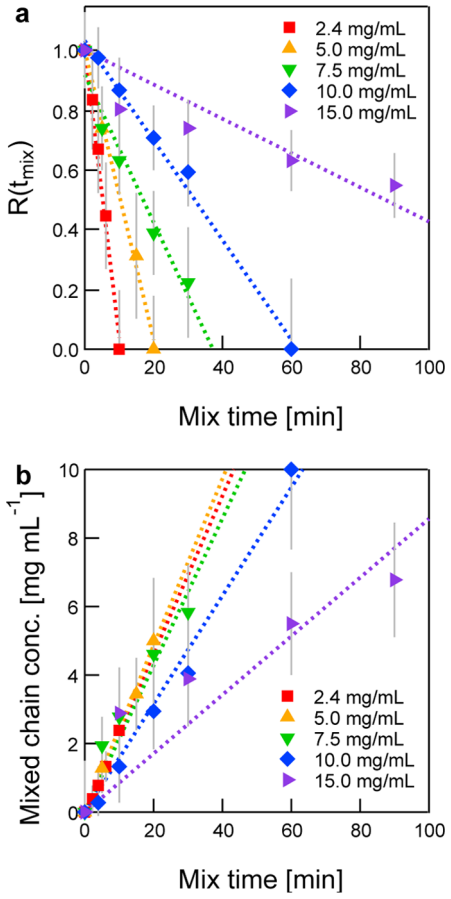

Figure 4. Quantification of chain exchange kinetics. (a) Extent of chain exchange $R(t_{mix})$ as a function of mix time at various polymer concentrations. (b) Concentration of randomly mixed chains as a function of mix time, for which the slopes are equal to the zero-order rate constant. Error bars represent the propagated uncertainty in the normalized scattered intensity based on the uncertainty in polymer concentration.

time (Figure 4a), further supporting a surface-limited exchange process.

Figure 4b shows the concentration of exchanged chains as a function of mix time by assuming that the chain exchange process followed a zero-order rate expression with respect to polymer concentration and mix time. The expression $[1 - R(t_{mix})]$ represents the fraction of chains exchanged as a function of mix time, and $c_0[1 - R(t_{mix})]$ represents the concentration of mixed chains, in which c_0 was the total constant polymer concentration. The corresponding zero-order rate constants were determined from the slopes of the linear fits shown in Figure 4b. The concentrations, rate constants, uncertainties, and coefficients of determination extracted from the linear fits are summarized in Table 1.

Interestingly, the rate constants decreased with increasing concentration, and the exchange kinetics for the highest examined polymer concentration (15 mg mL^{-1}) deviated somewhat from linearity. One possible explanation for these trends is that there are additional energetic penalties for chain exchange as polymer concentrations approach the semidilute regime. Previous work by Choi et al. examined the equilibrium kinetics of poly(styrene-*b*-ethylene-*alt*-propylene) micelles under quiescent conditions in squalane and found considerably slower single chain exchange kinetics at higher concentrations (15 vol %) compared to lower concentrations (0.5 to 2 vol %).[37] Their results later were supported with theoretical arguments by Halperin.[44] These arguments proposed that an additional osmotic penalty was incurred by overlapping corona chains, leading to increased energetic barriers for chain exchange at higher polymer concentrations. A similar argument could explain the concentration-dependent rate constant found

Table 1. Kinetic Parameters for Micelle Chain Exchange Induced by Rapid Vortex Mixing

concentration (mg mL^{-1})	rate constant (mg mL^{-1} min^{-1})	R^2
2.4 ± 0.1	0.23 ± 0.01	0.993
5.0 ± 0.1	0.24 ± 0.01	0.996
7.5 ± 0.1	0.23 ± 0.03	0.957
10.0 ± 0.1	0.15 ± 0.01	0.986
15.0 ± 0.1	0.09 ± 0.02	0.896

in this work; however, herein the concentrations were within the dilute regime (nearing the semidilute regime), and chain exchange did not occur readily in the bulk solution. An alternative macroscopic explanation could be that chain exchange was slowed due to an increased solution viscosity at higher polymer concentrations. Higher solution viscosities could potentially reduce the interface regeneration rate; however, the overall viscosity increase in the dilute solutions was expected to be negligible. Finally, bulk concentration has been shown to affect the adsorption kinetics of amphiphilic molecules[45] and nanoparticles[46] at the air–water interface. The decrease in the rate of chain exchange associated with increasing concentration could be due to slower micelle adsorption to the interface. Incorporating more controlled interfacial methodologies, as well as chain exchange studies in

dx.doi.org/10.1021/mz500435d | *ACS Macro Lett.* 2014, 3, 1106–1111

the semidilute and concentrated regime, are necessary to examine these hypotheses.

While the consequences of solution agitation on the stability of block polymer assemblies are largely unexplored, the results presented herein parallel reports on agitation-induced protein aggregation kinetics. Shear and interfacial effects are especially deleterious to protein stability, as proteins are known to aggregate at air−water interfaces.[30,32,34,49−52] For example, Bee et al. demonstrated that cyclic compression and expansion of the air−water interface led to aggregation of monoclonal antibodies, in which the mass and number of aggregates increased linearly with agitation time.[52]

Based on the linear kinetics found here, a similar surface-limited mechanism may lead to chain exchange in which block polymer micelles adsorb to an air−water interface, exchange some fraction of chains, and subsequently return back into the bulk solution when the interface collapses (Figure 5). It is likely

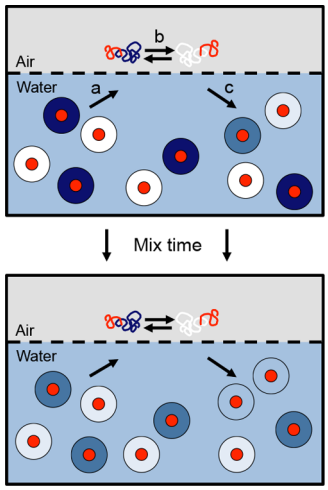

Figure 5. Schematic representation of proposed mechanism for agitation-induced chain exchange in which micelles (a) adsorb to the air−water interface, (b) exchange chains, and (c) are redispersed into the bulk solution. Given sufficient mix time, micelles eventually approach the randomly mixed condition with minimum scattering contrast.

that the micelles (rather than the individual block polymer chains) adsorb to the air−water interface due to the low concentration of free chains in the PB-PEO micelle solution.[47,48] Similarly, the direct adsorption of micelles to the air−water interface has been reported for nonionic micelle systems at concentrations much greater than the CMC; however, the exact mechanism of micelle adsorption and rearrangement at the air−water interface remains unknown.[47,48,53] In the present studies, it is uncertain whether single chains or some small fraction of chains are sequentially exchanged at the interface for each surface turnover cycle, that is, a cycle of micelle adsorption and redispersion. Nevertheless, these results have demonstrated that common mixing methods potentially can induce micelle chain exchange, even in a highly selective solvent. While additional studies are necessary to fully understand the coupled shear and interfacial effects on chain exchange and process time scales, the agitation-induced chain exchange presented here has critical implications in block polymer micelle stability and further emphasizes the importance of selecting and controlling processing conditions when preparing these assemblies.

■ ASSOCIATED CONTENT

Supporting Information

Experimental details, additional SANS data (Figure S1, Figure S3, and Table S1) and DLS data (Figure S2 and Table S2). This material is available free of charge via the Internet at http://pubs.acs.org.

■ AUTHOR INFORMATION

Corresponding Authors

*E-mail: msullivan@udel.edu.
*E-mail: thepps@udel.edu.

Author Contributions

†These authors contributed equally (R.P.M. and E.G.K.).

Notes

The authors declare no competing financial interest.

■ ACKNOWLEDGMENTS

The authors thank an Institutional Development Award (IDeA) from the National Institute of General Medical Sciences (NIGMS) of the National Institutes of Health (NIH), Grant P20GM103541, for financial support. The statements herein do not reflect the views of the NIH. E.G.K. also acknowledges support from a Department of Defense, Air Force Office of Scientific Research, National Defense Science and Engineering Graduate Fellowship, 32 CFR 168a. The authors acknowledge support of the National Institute of Standards and Technology (NIST), U.S. Department of Commerce, for providing the neutron facilities used in this work. University of Delaware (UD) Center for Neutron Science exploratory beam time was supported by NIST, U.S. Department of Commerce (#70NANB7H6178). The authors also thank Prof. Eric Furst and Dr. Paul Butler for helpful discussions and Dr. Yun Liu and Dr. Kathleen Weigandt for assistance with SANS measurements.

■ REFERENCES

(1) Alexandridis, P.; Hatton, T. A. *Colloids Surf., A* **1995**, *96*, 1−46.
(2) Alexandridis, P.; Lindman, B. *Amphiphilic Block Copolymers: Self Assembly and Applications*; Elsevier: Amsterdam, 2000.
(3) Patterson, J. P.; Cotanda, P.; Kelley, E. G.; Moughton, A. O.; Lu, A.; Epps, T. H.; O'Reilly, R. K. *Polym. Chem.* **2013**, *4*, 2033−2039.
(4) Vriezema, D. M.; Comellas Aragonès, M.; Elemans, J. A. A. W.; Cornelissen, J. J. L. M.; Rowan, A. E.; Nolte, R. J. M. *Chem. Rev.* **2005**, *105*, 1445−1490.
(5) Blanazs, A.; Armes, S. P.; Ryan, A. J. *Macromol. Rapid Commun.* **2009**, *30*, 267−277.
(6) Kelley, E. G.; Albert, J. N. L.; Sullivan, M. O.; Epps, T. H. *Chem. Soc. Rev.* **2013**, *42*, 7057−7071.
(7) Hayward, R. C.; Pochan, D. J. *Macromolecules* **2010**, *43*, 3577−3584.
(8) Meli, L.; Lodge, T. P. *Macromolecules* **2009**, *42*, 580−583.
(9) Meli, L.; Santiago, J. M.; Lodge, T. P. *Macromolecules* **2010**, *43*, 2018−2027.
(10) Lund, R.; Willner, L.; Stellbrink, J.; Lindner, P.; Richter, D. *Phys. Rev. Lett.* **2006**, *96*, 068302.
(11) Zinn, T.; Willner, L.; Lund, R.; Pipich, V.; Richter, D. *Soft Matter* **2012**, *8*, 623−626.
(12) Choi, S. H.; Lodge, T. P.; Bates, F. S. *Phys. Rev. Lett.* **2010**, *104*, 047802.
(13) Lu, J.; Bates, F. S.; Lodge, T. P. *ACS Macro Lett.* **2013**, *2*, 451−455.
(14) Lu, J.; Choi, S.; Bates, F. S.; Lodge, T. P. *ACS Macro Lett.* **2012**, *1*, 982−985.

(15) Halperin, A.; Alexander, S. *Macromolecules* **1989**, *22*, 2403−2412.
(16) Lund, R.; Willner, L.; Richter, D. *Adv. Polym. Sci.* **2013**, *259*, 51−158.
(17) Wang, Z.; Jiang, W. *Chem. Phys. Lett.* **2010**, *487*, 84−87.
(18) Yu, H.; Jiang, W. *Macromolecules* **2009**, *42*, 3399−3404.
(19) Cui, J.; Xu, J.; Zhu, Y.; Jiang, W. *Langmuir* **2013**, *29*, 15704−15710.
(20) Sorrells, J. L.; Tsai, Y.-H.; Wooley, K. L. *J. Polym. Sci., Part A: Polym. Chem.* **2010**, *48*, 4465−4472.
(21) Wang, C.-W.; Sinton, D.; Moffitt, M. G. *ACS Nano* **2013**, *7*, 1424−1436.
(22) Wang, C.-W.; Sinton, D.; Moffitt, M. G. *J. Am. Chem. Soc.* **2011**, *133*, 18853−18864.
(23) Stellbrink, J.; Lonetti, B.; Rother, G.; Willner, L.; Richter, D. *J. Phys.: Condens. Matter* **2008**, *20*, 404206.
(24) Kelley, E. G.; Murphy, R. P.; Seppala, J. E.; Smart, T. P.; Hann, S. D.; Sullivan, M. O.; Epps, T. H. *Nat. Commun.* **2014**, *5*, 4599.
(25) Kelley, E. G.; Smart, T. P.; Jackson, A. J.; Sullivan, M. O.; Epps, T. H. *Soft Matter* **2011**, *7*, 7094−7102.
(26) Won, Y. Y.; Davis, H. T.; Bates, F. S. *Macromolecules* **2003**, *36*, 953−955.
(27) Lund, R.; Willner, L.; Richter, D.; Dormidontova, E. E. *Macromolecules* **2006**, *39*, 4566−4575.
(28) Leal-Calderon, F.; Schmitt, V.; Bibette, J. *Emulsion Science: Basic Principles*; Springer: New York, 2007.
(29) Schuster, D. *Encylopedia of Emulsion Technology: Basic Theory, Measurement, Applications*; CRC Press: New York, 1987; Vol. 3.
(30) Thomas, C. R.; Geer, D. *Biotechnol. Lett.* **2011**, *33*, 443−456.
(31) Bai, G.; Bee, J. S.; Biddlecombe, J. G.; Chen, Q.; Leach, W. T. *Int. J. Pharm.* **2012**, *423*, 264−280.
(32) Kiese, S.; Papppenberger, A.; Friess, W.; Mahler, H.-C. *J. Pharm. Sci.* **2008**, *97*, 4347−4366.
(33) Nielsen, L.; Khurana, R.; Coats, A.; Frokjaer, S.; Brange, J.; Vyas, S.; Uversky, V. N.; Fink, A. L. *Biochemistry* **2001**, *40*, 6036−6046.
(34) Roberts, C. J. Nucleation, Aggregation, and Conformational Distortion. *Biophysical Methods for Biotherapeutics*; John Wiley & Sons, Inc.: Hoboken, NJ, 2014.
(35) Lund, R.; Willner, L.; Pipich, V.; Grillo, I.; Lindner, P.; Colmenero, J.; Richter, D. *Macromolecules* **2011**, *44*, 6145−6154.
(36) Lund, R.; Willner, L.; Richter, D.; Iatrou, H.; Hadjichristidis, N.; Lindner, P. *J. Appl. Crystallogr.* **2007**, *40*, S327−S331.
(37) Choi, S. H.; Bates, F. S.; Lodge, T. P. *Macromolecules* **2011**, *44*, 3594−3604.
(38) Choi, S. Y.; Bates, F. S.; Lodge, T. P. *J. Phys. Chem. B* **2009**, *113*, 13840−13848.
(39) Topel, Ö.; Çakır, B. A.; Budama, L.; Hoda, N. *J. Mol. Liq.* **2013**, *177*, 40−43.
(40) Kline, S. *J. Appl. Crystallogr.* **2006**, *39*, 895−900.
(41) Bijsterbosch, H. D.; de Haan, V. O.; de Graaf, A. W.; Mellema, M.; Leermakers, F. A. M.; Stuart, M. A. C.; Well, A. A. v. *Langmuir* **1995**, *11*, 4467−4473.
(42) Gonçalves da Silva, A. M.; Filipe, E. J. M.; d'Oliveira, J. M. R.; Martinho, J. M. G. *Langmuir* **1996**, *12*, 6547−6553.
(43) Zell, Z. A.; Isa, L.; Ilg, P.; Leal, L. G.; Squires, T. M. *Langmuir* **2013**, *30*, 110−119.
(44) Halperin, A. *Macromolecules* **2011**, *44*, 5072−5074.
(45) Yan, C.; Angus-Smyth, A.; Bain, C. D. *Faraday Discuss.* **2013**, *160*, 45−61.
(46) Schwenke, K.; Isa, L.; Del Gado, E. *Langmuir* **2014**, *30*, 3069−3074.
(47) Colegate, D. M.; Bain, C. D. *Phys. Rev. Lett.* **2005**, *95*, 198302.
(48) Song, Q.; Couzis, A.; Somasundaran, P.; Maldarelli, C. *Colloids Surf., A* **2006**, *282*−*283*, 162−182.
(49) Sluzky, V.; Tamada, J. A.; Klibanov, A. M.; Langer, R. *Proc. Natl. Acad. Sci. U.S.A.* **1991**, *88*, 9377−9381.
(50) Rudiuk, S.; Cohen-Tannoudji, L.; Huille, S.; Tribet, C. *Soft Matter* **2012**, *8*, 2651−2661.
(51) Wiesbauer, J.; Prassl, R.; Nidetzky, B. *Langmuir* **2013**, *29*, 15240−15250.
(52) Bee, J. S.; Schwartz, D. K.; Trabelsi, S.; Freund, E.; Stevenson, J. L.; Carpenter, J. F.; Randolph, T. W. *Soft Matter* **2012**, *8*, 10329−10335.
(53) Bhole, N. S.; Huang, F.; Maldarelli, C. *Langmuir* **2010**, *26*, 15761−15778.